

MRI evaluation of Kimura's disease with emphasis on diffusion weighted imaging and enhancement characteristics

Minhaj Shaikh, Pawan Garg, Parameshwar Sharma, Pushpinder Khara

Department of Diagnostic and Interventional Radiology, All India Institute of Medical Sciences, Jodhpur, Rajasthan, India

Correspondence: Dr. Minhaj Shaikh, Department of Diagnostic and Interventional Radiology, All India Institute of Medical Sciences, Jodhpur, Rajasthan, India. E-mail: minhaj0443@gmail.com

Abstract

Kimura's disease is a rare disease of the head and neck region affecting mainly the adult males in eastern countries. The parotid and periparotid subcutaneous regions are the most common sites in head and neck region. Coupled with peripheral eosinophilia and raised serum IgE levels as characteristic features on hemogram, a painless swelling in parotid and periparotid region is diagnostic of Kimura's disease. Magnetic resonance imaging (MRI) has been an important modality in evaluating lesions of the head and neck region. Recently, interest in the diffusion weighted imaging (DWI) and contrast enhanced MRI (CEMRI) imaging of lesions in Kimura's disease has been noted to characterize it and differentiate it from other pathologies. We describe a case a recurrent Kimura's disease of the periparotid region and its MRI features with special emphasis on its characteristics on DWI and contrast enhanced sequences.

Key words: Kimura's disease; diffusion weighted imaging; Contrast-enhanced magnetic resonance imaging; magnetic resonance imaging

Introduction

Kimura's disease is a chronic inflammatory disorder of the subcutaneous tissues of the head and neck region. Seen predominantly in the eastern hemisphere, its key pathologic feature is lymphoid follicles rich with eosinophils. Owing to its rare occurrence and clinico-radiologic similarity with various other common disease processes, it is a frequently misdiagnosed entity in the initial stages of evaluation. In the current era of high-volume cross-sectional imaging of head and neck pathologies, imaging appearance of Kimura's disease needs consideration. In this case report, we describe the magnetic resonance imaging (MRI) features in an adult male with Kimura's disease of the parotid region.

Case Report

A 36-year-old man presented with gradually progressive recurrent painless swelling in the right postauricular region for the past 1 year. He had a similar swelling 10 years back, which was operated upon and confirmed to be Kimura's disease on histopathologic examination of the excised specimen. At present, the hemogram revealed elevated eosinophil count (relative eosinophil count of 14.9% and absolute eosinophil count of 750 cells per microliter). In this case of recurrent Kimura's disease involving the right parotid region, multiplanar and multisequence contrast-enhanced MRI was done on a 3.0 T MRI scanner

This is an open access journal, and articles are distributed under the terms of the Creative Commons Attribution-NonCommercial-ShareAlike 4.0 License, which allows others to remix, tweak, and build upon the work non-commercially, as long as appropriate credit is given and the new creations are licensed under the identical terms.

For reprints contact: reprints@medknow.com

Cite this article as: Shaikh M, Garg P, Sharma P, Khara P. MRI evaluation of Kimura's disease with emphasis on diffusion weighted imaging and enhancement characteristics. Indian J Radiol Imaging 2019;29:215-8.

Access this article online

Quick Response Code:



Website:
www.ijri.org

DOI:
10.4103/ijri.IJRI_468_18

(Discovery™ MR750, GE Healthcare, Milwaukee, USA). After the acquisition of routine sequences, intravenous injection of gadodiamide at a dose of 0.1 mmol/kg was administered and three-dimensional (3D) fat-suppressed T1-weighted sequences were acquired at 4 and 20 min after contrast injection.

The axial T2-weighted images showed a predominantly hyperintense, heterogenous infiltrative lesion located posterior to the right parotid gland and infiltrating into its posterior border [Figure 1]. Few tiny signal intensity voids were noted within this lesion, indicative of vessels. There was no deeper infiltration beyond the subcutaneous plane; however, multiple associated enlarged and hyperintense lymph nodes were noted in the right posterior cervical region (level V). Enlarged intraparotid lymph nodes were also noted. On evaluating the diffusion weighted images (DWI) at b value of 1000 s/mm², the subcutaneous lesion showed increased signal intensity compared to the normal parotid gland [Figure 2]. On DWI, the associated intraparotid and cervical lymph nodes showed homogeneously increased signal intensity, which was higher than the subcutaneous periparotid lesion. On corresponding apparent diffusion coefficient (ADC) maps, the degree of hypointensity of the lymph nodes was more compared to the subcutaneous periparotid lesion. The

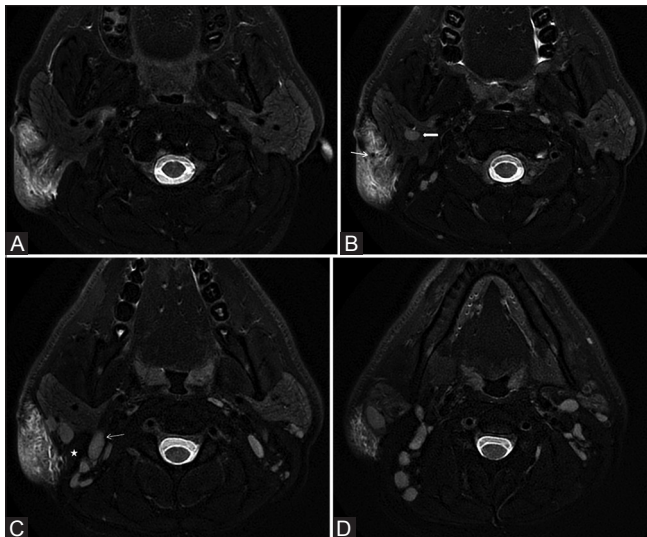


Figure 1 (A-D): Axial T2 weighted images. (A) A heterogeneously hyperintense subcutaneous lesion is noted in the right posterior periparotid region with indistinct posterior margin of the parotid gland along the line of contact, suggestive of early infiltration. (B) Small circular and tubular signal voids are seen within the subcutaneous lesion due to vessels within it (*thin white arrow*). Also note the enlarged intraparotid lymph node (*block white arrow*). (C) The enlarged and homogeneously hyperintense posterior cervical lymph nodes can be seen (*thin white arrow*). Note the normal size and signal intensity of the right sternocleidomastoid muscle (*white star*) separating the subcutaneous lesion and the enlarged posterior cervical lymph nodes confirming the lack of deeper infiltration of the subcutaneous lesion. (D) An entire chain of enlarged and hyperintense right-sided posterior cervical lymph nodes can be seen deep to the sternocleidomastoid muscle

mean values and standard deviation of the ADC values of the subcutaneous lesion and lymphadenopathy were 1.76 ± 0.142 and 0.812 ± 0.06 mm²/s respectively. The contrast-enhanced images acquired at 4 and 20 min after contrast injection showed significant difference between the two entities [Figure 3]. The subcutaneous lesion showed progressively increasing enhancement on comparing the 4 and 20 min post contrast images. The lymphadenopathy, on the contrary, showed progressive fading of contrast enhancement at 20 min.

Discussion

The earliest description of Kimura's disease dates back to 1948 when Kimura *et al.* described it as an unusual granulation tissue associated with lymphatic hyperplasia.^[1] The pathologic lesion consists of follicles comprising eosinophils, plasma cells, lymphocytes, and mast cells with associated proliferation of vessels and fibrosis of the stroma.^[2] It usually affects Asian males in second, third, and fourth decade.^[1] The most common presentation is painless, single or multiple subcutaneous nodules in the head and neck region, most often in the parotid and submandibular location.^[3] Rarely, other sites such as parapharyngeal space can also be involved.^[4] The associated key features which are highly valuable in making a clinical diagnosis is peripheral eosinophilia (10–70%) and raised serum IgE level (800–35,000 IU/mL).^[3,5]

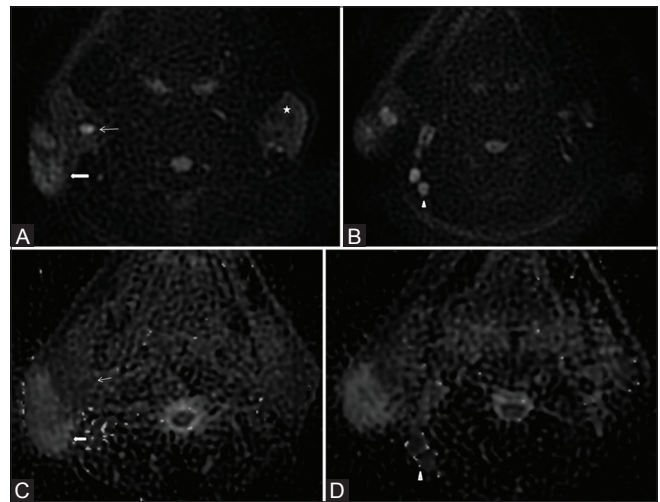


Figure 2 (A-D): Diffusion weighted images and ADC maps. (A and B) The signal intensity of the subcutaneous lesion (*block white arrow*) is higher than the normal parotid gland parenchyma (*star*) on both sides but less than that of the disease associated enlarged right intraparotid (*thin white arrow*) and right posterior cervical (*block arrowhead*) lymph nodes. (C and D) The ADC maps corresponding to the DWI in (A) and (B) show most marked hypointensity (*reduced ADC values*) in the enlarged right intraparotid (*thin white arrow*) and posterior cervical (*block arrowhead*) lymph nodes. Thus, the disease associated enlarged lymph nodes in the Kimura's disease show homogenous diffusion restriction. The subcutaneous lesion (*block white arrow*), however, does not show lower ADC values (*rather appears bright*) than the normal parotid glands and lymph nodes

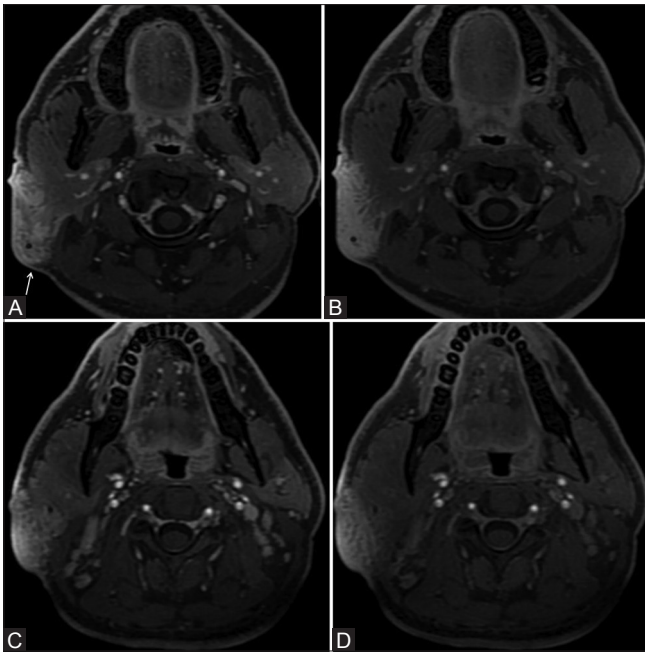


Figure 3 (A-D): Contrast enhanced T1 weighted images. (A) Mild enhancement of the subcutaneous lesion (*thin white arrow*) at 4 min after contrast injection. (B) Image at the same level 20 min after contrast injection shows increased enhancement within the subcutaneous lesion. (C) Moderate homogenous enhancement of the enlarged lymph nodes at 4 min after contrast injection. (D) At 20 min postcontrast injection, the enlarged lymph nodes show reduced and heterogeneous enhancement (progressive washout). The subcutaneous lesion shows progressive delayed enhancement over time while the lymph nodes show progressive washout of enhancement

This characteristic constellation of features—mass-like inflammatory lesion in periparotid region, peripheral eosinophilia, and raised serum IgE levels—is the basis of clinical diagnosis of Kimura's disease.

MRI and computed tomography (CT) are the key imaging modalities in Kimura's disease. Majority of the lesions in Kimura's disease occur in proximity to parotid gland, either within its parenchyma or within the periparotid subcutaneous space and infiltrating into the parotid gland parenchyma.^[6] In two large case series evaluating the CT and MRI features of Kimura's disease, two morphological patterns of the lesions were noted; that is, well-defined nodular pattern and ill-defined infiltrative or plaque-like pattern.^[7,8] The infiltrative or plaque-like morphology was far more common than the well-defined nodular pattern, both occurring in these studies at 84 and 98%, respectively.^[7,8] The MRI signal intensity of these lesions was variable on T1-weighted images and predominantly hyperintense on T2-weighted images.^[7-9] On contrast-enhanced CT and MRI images, the pattern of enhancement is variable in terms of degree of enhancement and heterogeneity, owing to varying degrees of stromal fibrosis and vascular proliferation. However, a relatively homogenous pattern and intense or marked enhancement has been reported in majority of cases.^[7-9] Some authors describe intense enhancement as a classical feature of Kimura's

disease.^[6] Another interesting feature of Kimura's lesion is the presence of serpentine signal intensity void areas on T2 and contrast-enhanced images, as seen in our case. These are due to prominent vascular structures in the lesion owing to pathologic vascular proliferation.^[8]

The role of DWI in Kimura's disease has been explored in recent years.^[10,11] The differential signal intensity of the subcutaneous parotid/periparotid Kimura's lesion and the associated lymphadenopathy is an important characteristic feature on DWI. There is heterogeneous and intermediately high signal intensity of the subcutaneous Kimura's lesion and markedly high signal intensity of the associated lymphadenopathy on DWI. Correspondingly, the ADC values of subcutaneous parotid/periparotid lesion are higher compared to the ADC values of the involved lymph nodes. Relative hypercellularity of the lymph nodes is considered to be the cause of its high signal intensity on DWI. The role of dynamic contrast-enhanced MRI in Kimura's disease has been studied by Horikoshi *et al.* in seven patients.^[10] They studied the time-intensity curves of enhancement in the subcutaneous Kimura's lesion and the associated involved lymph nodes. They found that the subcutaneous Kimura's lesions showed gradual upward or progressive delayed enhancement, while the associated lymphadenopathies showed early enhancement. The presence of fibrosis in the subcutaneous lesion is considered to be the cause for its progressive delayed enhancement.^[10] The differential imaging features of subcutaneous lesion and the associated lymphadenopathy on dynamic contrast-enhanced MRI and DWI are characteristic and have been demonstrated to be useful in differentiating Kimura's disease from other commoner and more sinister pathologies of head and neck, especially malignant lymphoma.^[10,11] Wang *et al.* have also investigated the role of magnetic resonance spectroscopy in characterizing Kimura disease. They found relatively high choline/creatine ratios in the involved lymph nodes and relatively low choline/creatine ratios in the subcutaneous lesion.^[11]

Although the confirmatory diagnosis of Kimura's disease is pathological, the differential behavior of subcutaneous parotid/periparotid lesion and the associated lymphadenopathy on MRI, especially DWI and contrast-enhanced MRI are of great importance in its noninvasive diagnosis.

Informed consent

Written informed consent for medical information and images to be published in this case report was provided by the patient.

Declaration of patient consent

The authors certify that they have obtained all appropriate patient consent forms. In the form the patient has given

his consent for his images and other clinical information to be reported in the journal. The patient understands that his name and initials will not be published and due efforts will be made to conceal his identity, but anonymity cannot be guaranteed.

Financial support and sponsorship

Nil.

Conflicts of interest

There are no conflicts of interest.

References

1. Kimura T, Yoshimura S, Ishikawa E. Unusual granulation combined with hyperplastic changes of lymphatic tissue [in Japanese]. *Trans Soc Pathol Jpn* 1948;37:179-80.
2. Ishikawa E, Tanaka H, Kakimoto S, Takasaki S, Kirino Y, Sakata A, *et al.* A pathological study on eosinophilic lymphfolliculoid granuloma (Kimura's disease). *Acta Pathol Jpn* 1981;31:767-81.
3. Chen H, Thomson LD, Aguilera NS, Abbondanzo SL. Kimura disease: A clinicopathologic study of 21 cases. *Am J Surg Pathol* 2004;28:505-13.
4. Keng CG, Pang KP, Teng PW. Kimura's disease of the parapharyngeal space. *Ear Nose Throat J* 2006;85:106-08.
5. Takahashi S, Ueda J, Furukawa T, Tsuda M, Nishimura M, Orita H, *et al.* Kimura disease: CT and MR findings. *AJNR Am J Neuroradiol* 1996;17:382-85.
6. Som PM, Brandwein MS. Salivary glands: Anatomy and pathology. In: Som PM, Curtin HD, editors. *Head and Neck Imaging*. 4th ed, vol 2. St Louis: Mosby; 2003. p. 2121-2.
7. Gopinathan A, Tan TY. Kimura's disease: Imaging patterns on computed tomography. *Clin Radiol* 2009;64:994-9.
8. Park SW, Kim HJ, Sung KJ, Lee JH, Park IS. Kimura disease: CT and MR imaging findings. *AJNR Am J Neuroradiol* 2012;33:784-8.
9. Zhang R, Ban XH, Mo YX, Lv MM, Duan XH, Shen J, *et al.* Kimura's disease: The CT and MRI characteristics in fifteen cases. *Eur J Radiol* 2011;80:489-97.
10. Horikoshi T, Motoori K, Ueda T, Shimofusa R, Hanazawa T, Okamoto Y, *et al.* Head and neck MRI of Kimura disease. *Br J Radiol* 2011;84:800-4.
11. Wang J, Tang Z, Feng X, Zeng W, Tang W, Wu L, *et al.* Preliminary study of diffusion-weighted imaging and magnetic resonance spectroscopy imaging in Kimura disease. *J Craniofac Surg* 2014;25:2147-51.